IOPscience iopscience.iop.org

Home Search Collections Journals About Contact us My IOPscience

Diffraction and transmission of light in low-refractive index Penrose-tiled photonic quasicrystals

This article has been downloaded from IOPscience. Please scroll down to see the full text article.

2001 J. Phys.: Condens. Matter 13 10459

(http://iopscience.iop.org/0953-8984/13/46/314)

View the table of contents for this issue, or go to the journal homepage for more

Download details:
IP Address: 171.66.16.226
The article was downloaded on 16/05/2010 at 15:09

Please note that terms and conditions apply.

INSTITUTE OF PHYSICS PUBLISHING JOURNAL OF PHYSICS: CONDENSED MATTER

J. Phys.: Condens. Matter **13** (2001) 10459–10470 PII: S0953-8984(01)27526-2

Diffraction and transmission of light in low-refractive index Penrose-tiled photonic quasicrystals

M A Kaliteevski[1,2], S Brand[1], R A Abram[1], T F Krauss[3], P Millar[4] and R M De La Rue[4]

[1] Department of Physics, University of Durham, South Road, Durham DH1 3LE, UK
[2] Groupe d'Etude des Semiconducteurs CC074, Universite Montpellier II, Place Bataillon 34095, Cedex 05, France
[3] School of Physics, University of St Andrews, St Andrews, Fife KY16 9SS, UK
[4] Department of Electronic and Electrical Engineering, University of Glasgow, Glasgow G12 8LT, UK

Received 1 August 2001, in final form 11 September 2001
Published 2 November 2001
Online at stacks.iop.org/JPhysCM/13/10459

Abstract

We report the measurements of the diffraction pattern of a two-dimensional Penrose-tiled photonic quasicrystal, obtained by etching air cylinders in a silica substrate, and the modelling of the light propagation and dispersion relations of photons inside such a structure. The calculated transmission spectra exhibit dips whose positions are insensitive to the direction of propagation and whose depth increases with increasing structure length. An approach is developed for the calculation of the dispersion relations which is based on a set of reciprocal vectors defined by the diffraction pattern. The dispersion curves exhibit gap-like features at frequencies corresponding to the dips in the transmission spectra.

1. Introduction

Photonic crystals have attracted considerable interest in the last decade due to their ability to inhibit the spontaneous emission of light and other potential applications in various optoelectronic devices [1–4]. Photonic bands originate from the multiple diffraction of light due to the varying dielectric constant of the material. Only evanescent electromagnetic modes are possible in the photonic bandgap and this feature can be used to advantage in mirrors for optical microcavities and waveguides. However, the highest level of rotational symmetry in crystals is six, and even in such structures the position of gaps for different directions in the Brillouin zone can differ substantially. The level of rotational symmetry possible is greater if one includes quasicrystals [5], which were discovered experimentally by Shechtman *et al* [6]. Analysis of the properties of eight-fold [7, 8], ten-fold [9, 10] and 12-fold [11, 12] photonic quasicrystals has shown that a gap in the density of modes, accompanied by significant dips in the transmission spectra can be achieved in such structures, even when the refractive index

 © 2001 IOP Publishing Ltd Printed in the UK

contrast of the materials used in such structures is not very high, as for example in the case of silicon nitride and air.

The bandstructure of quasicrystals has a more complicated nature than that for true crystals. For the latter, a Bloch theorem for the electromagnetic field exists, and such terms as propagating states, Bloch wavevector, bandgap and attenuation length have clear physical meanings and can even be directly measured experimentally. Some concepts developed for crystals can be used for the analysis of the properties of quasicrystals, although for quasicrystalline systems a Bloch theorem does not exist. For example dispersion relations for the photonic Fibonacci lattices have been experimentally measured [13], and gaps in the dispersion relations, corresponding to the dips in the transmission spectra, have been obtained.

The analysis of the bandstructure of quasicrystals has been the subject of numerous investigations. For one-dimensional quasicrystals in the form of Fibonacci lattices it has been shown that the mode spectrum is a Cantor set for which the gaps can be enumerated [14, 15]. A recent study of the transmission of light in photonic Fibonacci lattices has revealed that a minimum size of the system is required for the formation of a 'true' gap, where light decays exponentially with increase of system size [16]. A method for calculating the bandstructure of two- and three-dimensional quasicrystals resulted from the discovery that the original reciprocal vectors (RVs) can be replaced with their rational approximants and the bandstructure analysed inside the pseudo-Jones zone; the polygon in the reciprocal space obtained by bisecting the basic RV [17, 18]. An alternative approach has recently been introduced and used for the analysis of the bandstructure of Fibonacci lattices. It is based on an analysis of the branches oriented along the free-photon dispersion line and uses a true set of RVs for the calculation of dispersion relations [16]. The gaps positions and widths predicted using this approach coincide with the results obtained using a conventional transfer matrix method.

The aim of this work is to investigate the optical properties of Penrose-tiled photonic crystals [19] possessing ten-fold symmetry and, in particular, the possibility of the application of an approach based on a kind of extended zone scheme in reciprocal space for the calculation of the density of modes in two-dimensional quasicrystals. The quasicrystalline structure considered is obtained by tiling the plane with two kinds of rhombus: a thin tile (with vertex angles 36° and 144°) and a fat tile (72° and 108°), as shown in figure 1. Air cylinders, placed at the vertices form the physical structure. The tiling was generated using the method described by Janssen [20], which involves projecting a cubic lattice in six dimensions onto the tiling plane. In the case considered here, the tiling plane contains a generating lattice point, resulting in the structure having particular symmetry properties, including a centre of ten-fold rotational symmetry.

2. Diffraction of light

The sample for the diffraction experiment, shown in figure 2, was fabricated using electron-beam lithography. A silica substrate was first coated with 30 nm of titanium, then with a 900 nm layer of UV3 resist. After patterning, the air cylinders were etched using CHF_3. The depth of the cylinders was about 700 nm. Finally, the titanium coating was removed using high-field evaporation. The size of the patterned area is about 120×110 μm and contains 121 cylinders. The diameter of the cylinders is about 3 μm and the value of the tile side used for the patterning was l0 μm. Note that the experimental sample is only a fraction of the structure, shown in figure 1 and does not contain a centre of rotational symmetry.

A He–Ne laser, with a wavelength of 633 nm and Gaussian-shaped beam, was collimated to provide a beam diameter of about 130 μm, matching the size of the patterned area. The laser beam was incident normal to the sample, and produced a diffraction pattern on a screen

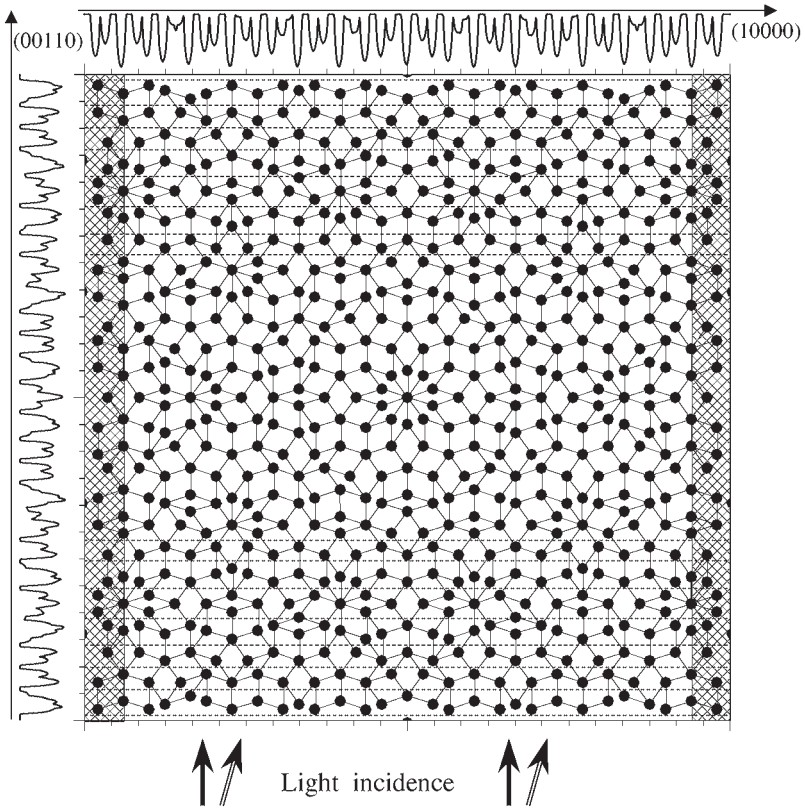

Figure 1. Schematic view of the Penrose structure, obtained using thin and thick tiles. The black circles placed at the vertices of the tiling correspond to air cylinders. The hatched areas indicate the left and right boundaries, where periodic boundary conditions (required for the transmission calculation) can be set up without breaking the tiling near the boundary. Horizontal dashed lines indicate the slices of the structure of different thickness for which transmission spectra were calculated. The profiles at the sides the boundaries of the structure exhibit the profile of the dielectric constant, averaged in the cross section perpendicular to the specific direction.

placed 24 cm behind the sample, as shown in figure 3. The diffraction pattern possesses ten-fold rotational symmetry, and contains a series of spots of different intensity, surrounding the central undiffracted beam. These spots can be associated with vectors in reciprocal space, which we will call 'RVs'.

Contrary to the case of a periodic crystal, the indexing of the diffraction pattern of aperiodic quasicrystals is not a trivial task, due to the self-similarity of the structure. The RVs of a periodic structure form the periodic reciprocal lattice and we can always find a set of primitive RVs of minimum magnitude whose linear combinations generate the entire reciprocal lattice. However, in aperiodic quasicrystals the RVs densely fill all reciprocal space, and it is not possible to choose any RVs of minimum magnitude. Nevertheless, it turns out to be convenient to choose some basic RVs that correspond to relatively intense spots in the diffraction pattern, and have magnitudes that are related to the inverse of certain lengths in the structure, such as a tile side [20].

Figure 4 shows a photograph of the diffraction pattern of the experimental structure, with only three series of the most intensive spots visible. The magnitude and orientation of the

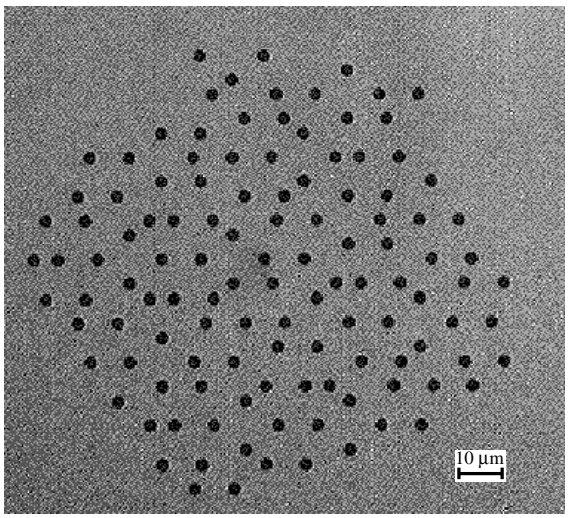

Figure 2. Micrograph of the sample used in the diffraction experiment.

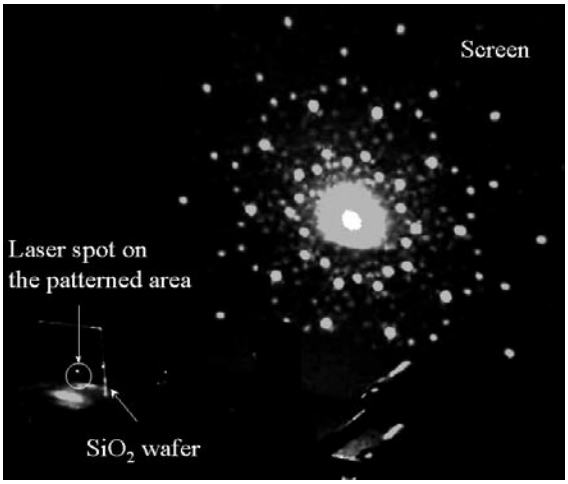

Figure 3. General photograph of the experimental diffraction pattern.

RVs of the internal series correspond to the inverse of half the long diagonal of the thin tile. Similarly, the middle series corresponds to half the long diagonal of the thick tile and the external series corresponds to half of that tile side length.

We choose the RVs for the internal series of spots to form a basic set, which we denote by $\pm \boldsymbol{F}_i$ ($i = 1, 5$), where

$$\boldsymbol{F}_1 = (1, 0) = (10000)$$
$$\boldsymbol{F}_2 = (\cos(\pi/5), \sin(\pi/5)) = (01000)$$
$$\boldsymbol{F}_3 = (\cos(2\pi/5), \sin(2\pi/5)) = (00100)$$
$$\boldsymbol{F}_4 = (\cos(3\pi/5), \sin(3\pi/5)) = (00010)$$
$$\boldsymbol{F}_5 = (\cos(4\pi/5), \sin(4\pi/5)) = (00001).$$

In these equations, the vectors are expressed in both conventional two-dimensional Cartesian coordinates and a symbolic five-dimensional vector notation. The magnitude of each $\boldsymbol{F}_i$ is related to the tile side length d as $|\boldsymbol{F}_i| = 2\pi/(d\cos(\pi/10)) \approx 1.051 \times 2\pi/d$. In the

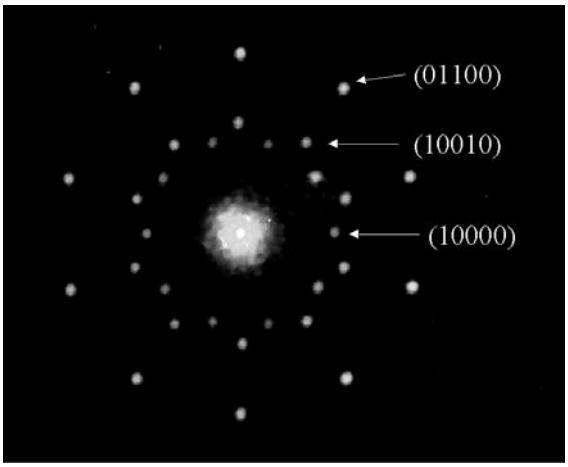

Figure 4. Photograph of the most pronounced peaks on the experimental diffraction pattern and indexing of the diffraction pattern.

subsequent discussion we use $|\boldsymbol{F}_i|$ as the unit of length in the reciprocal space. When we have chosen the basic set of RVs, it is possible to index the entire diffraction pattern. The intensities of the diffraction peaks related to the different prominent series, their indexes and the related elements of the tiles defining the quasicrystal, are shown in table 1. It can be seen that the most intense features are related to those RVs that can be represented as 'symmetric' linear combinations with small coefficients of the basic RVs, such as (10000), (10010), (11000), ... It can also be seen that the strongest diffraction peaks corresponds to two kinds of direction: either a basic set, (10000), (11011), (11100); or 18° off, (10010), (11000), (11110). The intensities of the peaks decrease rapidly as the number of basic RVs used increases, or with departure from the two directions specified above. However, there are exceptions to this rule, such as the diffraction spot corresponding to RV (10100) which has very small intensity.

Figure 5 shows the calculated Fourier representation of the distribution of the dielectric constant in the structure, shown in figure 1. The picture, in general, reproduces the measured diffraction pattern, but additional series of spots can be seen, such as the 'deflated' (10001), (11-101) and minor features, such as (30-110) and (111-1-1).

The electromagnetic power of the experimentally measured diffraction spots, and the magnitude of the calculated Fourier coefficients, are shown in table 1. Note, that the relative power of the spots correspond closely to the squared magnitude of Fourier coefficients.

3. Transmission of light

If a light wave propagates in a photonic crystal, for which the spatially varying dielectric constant has a substantial Fourier coefficient related to some RV $\boldsymbol{g}$, the wave can be reflected back if the magnitude of its wavevector $|\boldsymbol{K}|$ (which is approximately $\langle\sqrt{\varepsilon}\rangle\omega/c$) is equal to $|\boldsymbol{g}|/2$. This can be physically understood in terms of Bragg reflections from crystalline planes. Such reflection leads to the formation of the gaps in the mode spectrum and the intensity of the light decays exponentially as it propagates through the structure. In the quasicrystalline structure, shown in figure 1, one can also consider plane-like sequences of the air cylinders, which are illustrated by the profiles of the dielectric constant, averaged in the cross section perpendicular to the particular direction. For the structure under study, possessing an average refractive index $\langle\sqrt{\varepsilon}\rangle \approx 1.4$, the frequencies f of the possible gap should satisfy the relation

$$\frac{fd}{c} \approx \frac{1.05}{2\langle\sqrt{\varepsilon}\rangle}\frac{g}{F} \tag{1}$$

Table 1. Magnitudes of different Fourier coefficients of the Penrose structure and intensities of the diffracted beams.

		Intensity		Related value, normalized to those for (10000)		
RV	Magnitude	Magnitude of Fourier coefficient	Power of the spots (μW)	Magnitude of Fourier coefficient squared	Power of the spots	The element of the tile, which can be associated with RV
(00000)	0.000	0.5294	1270	29	190	
(10001)[a]	0.618	0.0036	Not pronounced	0.2	—	
(11-101)	0.726	0.0034	Not pronounced	0.18	—	
(10000)[a]	1.000	0.018	6.7	1.00	1.00	Half of the long diagonal, thin tile
(10010)	1.176	0.02	8.3	1.23	1.23	Half of the long diagonal, thick tile
(10100)[a]	1.618	<0.001	Not pronounced	<0.0004	—	Half of the short diagonal, thick tile
(11000)	1.902	0.023	12.7	1.69	1.89	Half of the tile side
(1010-1)	2.149	0.0067	0.9	0.14	0.13	
(11011)[a]	2.236	0.0074	1.4	0.16	0.21	
(30-110)[a]	2.381	0.0023	Not pronounced	0.017	—	
(11100)[a]	2.618	0.0073	1.6	0.16	0.24	
(11110)	3.078	0.0082	1.8	0.20	0.27	Half of the short diagonal, thin tile
(111-1-1)[a]	3.236	0.002	Not pronounced	0.11	—	

[a] Denotes RVs which are oriented as the basic RVs $\boldsymbol{F}_i$.

which gives the value of $fd/c \approx 0.37$ for the scattering by the RV (10000) and the value of $fd/c \approx 0.44$ for the scattering by the vector (10100). The maximum deviation from the symmetry direction in the structure, possessing ten-fold rotational symmetry is 18°, and it can be argued that the gap frequency will be altered by no more than approximately a factor of $\cos 18^\circ \approx 0.95$.

Figure 6 shows the calculated transmission spectra of light propagating through fragments of the structure of different size as shown in figure 1. Each such fragment includes the centre of the structure and its boundaries are shown as dashed curves. The refractive indices of the materials and the cylinder radius are the same as for the experimental sample shown in figure 2. The calculational method is based on a combination of transfer matrix and multiple scattering techniques, and was performed using the publicly available code of Bell *et al* [21] after suitable modification. This method facilitates calculation of the propagation of light through a structure with a two-dimensional spatial variation of the dielectric constant, and with periodic boundary conditions on the lateral (left and right) boundaries of the structure. An infinite Penrose structure of the type considered does not obey such periodic boundary conditions, and taking an arbitrary length of the structure in the (00110) direction and repeating it laterally would result in a discontinuity of the tiling where the pieces meet. However, in the structure of finite size

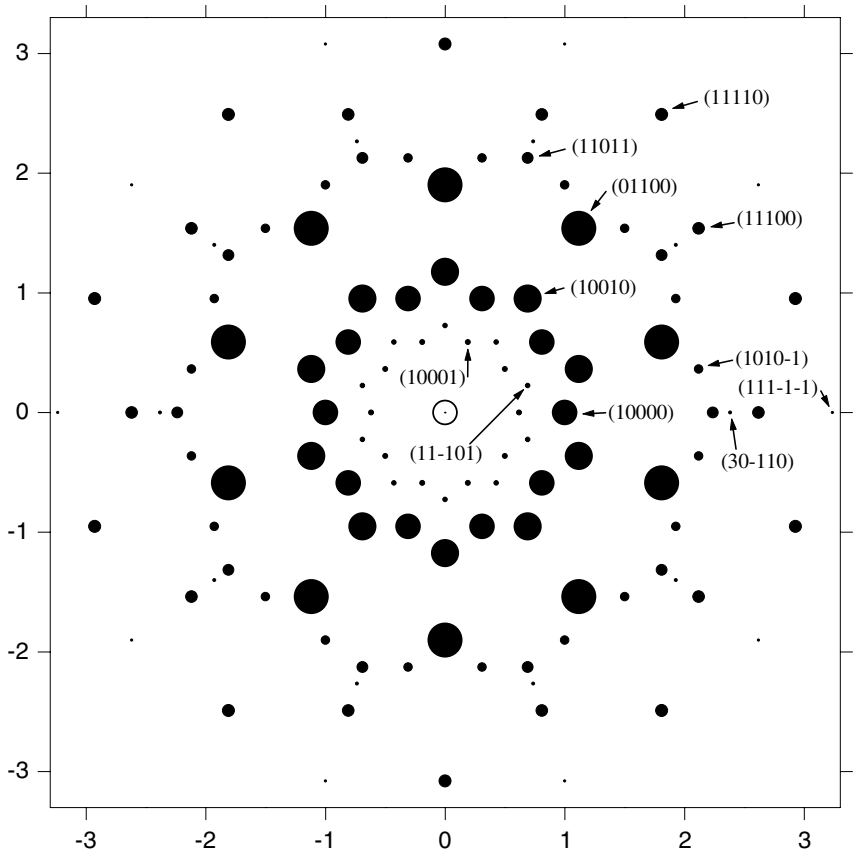

Figure 5. Fourier transform of the dielectric constant distribution in the Penrose-tiled quasicrystal. The radius of the spot is proportional to the magnitude of the related Fourier coefficient.

under study, we can find rectangular regions of the type illustrated in figure 1 which, if repeated laterally, will produce a structure without any tiling discontinuity. It must be emphasized, that the infinitely wide structure obtained will not reproduce the true Penrose tiling, but will have properties representative of it. The calculations were performed for the E-polarization (when the electric field is parallel to the cylinders) and H-polarization (when the magnetic field is parallel to the cylinders).

The spectra for two directions of propagation (along (00110), when light is incident normally, and along (00100), which is 18° off normal incidence) and both the E- and H-polarizations, exhibit two dips at the frequencies $fd/c \approx 0.37$ and $fd/c \approx 0.46$, which correspond well to our approximate estimates given above. The positions of the dips do not depend on the thickness of the sample, which is unambiguous evidence of gap-like features in the mode spectrum. The spectra for the H-polarization for the direction (00110) are similar to the spectra for the E-polarization for the direction (00100), and vice versa. The relative width of the lower frequency and higher frequency dips are about 2 and 5%, respectively.

Figure 7 shows the dependence of the minimum transmission coefficient at the dips as a function of the sample length for the different polarizations and directions of propagation, and illustrates the attenuation of light propagating through the Penrose structure. Since the transmission coefficient for the minima is in the range of 0.1–0.2 for the structure of

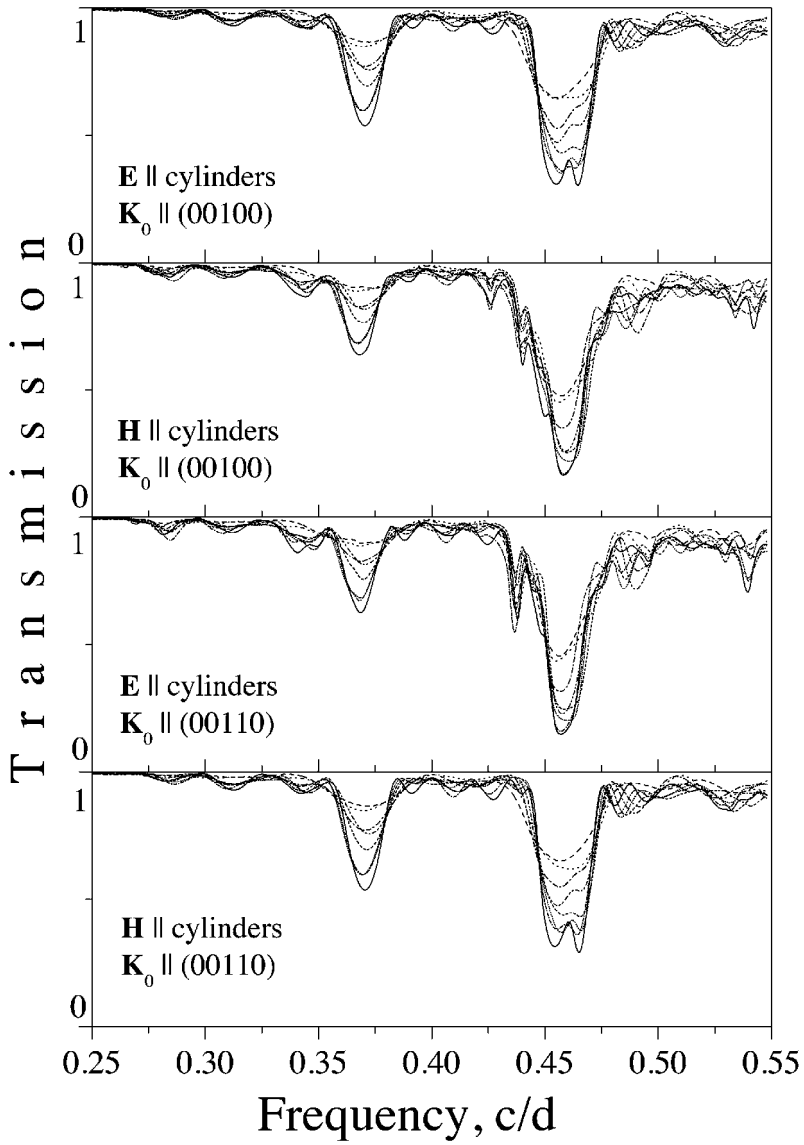

Figure 6. Calculated transmission spectra of the E- and H-polarized waves for two directions of propagation; along (00110), perpendicular to the boundary of the structure, shown in figure 1, and along the basic RV (00100), 18° off the normal to the boundary of the structure. Different curves correspond to the slices of the structure of different thickness: dashed, 10.6d; dotted, 12.14d; dash-dot, 14.26d; dash-dot-dot, 16.6d; short dash, 18.3d; short dot, 20.2d; short dash-dot, 21.7d; solid, 23.6d.

largest length, we cannot make the conclusion on nature of this decay, but the dependence of transmission on the sample length corresponds to an exponential decay with attenuation lengths 12d, 16d, 28d and 36d. Such behaviour indicates the existence of a gap for all directions and both polarizations. Although the attenuation length for the Penrose structure is much larger than for the same air cylinders arranged in a square or hexagonal pattern, gaps exist for all directions and polarizations [22].

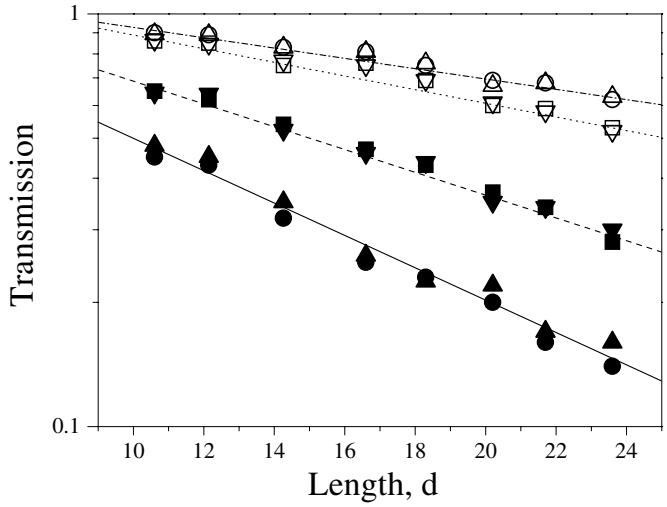

Figure 7. The dependence of the calculated transmission coefficient at the dips in the spectra of figure 6 for different directions of light incidence and polarization. Square, H-polarization (00110); circle, E-polarization, (00110) direction; up-triangle, H-polarization, (00100) direction; down-triangle, E-polarization, (00100) direction; open symbols correspond to the dip at the frequency of $fd/c \approx 0.37$ and solid symbols corresponds to the dips at the frequency of $fd/c \approx 0.46$. Solid, dashed, dotted and dash-dotted curves represent exponential fits with attenuation lengths of $12d$, $16d$, $28d$ and $36d$, respectively.

4. Dispersion relations

A number of procedures for the calculation of the bandstructure of photonic crystals are well established [23]. Consider a two-dimensional photonic structure, comprising cylinders oriented along the z-axis and with the dielectric constant $\varepsilon(\rho) = \varepsilon(\boldsymbol{e}_x x + \boldsymbol{e}_y y)$ defined as a function of the two Cartesian coordinates x and y. An electromagnetic field propagating in the x–y plane can be represented as a superposition of fields with two independent polarizations; the H-polarization (with the magnetic field oriented parallel to the cylinders and field components (E_x, E_y, H)) and the E-polarization (with the electric field oriented parallel to the cylinders and field components (H_x, H_y, E)).

In the case of the H-polarization, the electromagnetic field component H varying with frequency ω must satisfy the wave equation

$$\frac{\partial}{\partial x}\left(\frac{1}{\varepsilon}\frac{\partial H}{\partial x}\right) + \frac{\partial}{\partial y}\left(\frac{1}{\varepsilon}\frac{\partial H}{\partial y}\right) + \frac{\omega^2}{c^2}H = 0. \tag{2}$$

To solve this equation we make a Fourier expansion of $\varepsilon^{-1}(\rho)$ and $H(\rho)$ such that

$$\frac{1}{\varepsilon(\rho)} = \sum_{\boldsymbol{g}_i} \tilde{\varepsilon}(\boldsymbol{g}_i) \exp(\boldsymbol{g}_i \cdot \rho) \tag{3}$$

$$H(\rho, \omega) = \sum_{\boldsymbol{g}_i} A(\boldsymbol{k}, \boldsymbol{g}_i) \exp(\mathrm{i}(\boldsymbol{k} + \boldsymbol{g}_i) \cdot \rho) \tag{4}$$

where the $\boldsymbol{g}_i$ are the reciprocal lattice vectors of the crystal and $\boldsymbol{k}$ is the two-dimensional wavevector of the wave in the x–y plane. Note that the field H has the form of a Bloch wave, and $\boldsymbol{k}$ can always be chosen to lie in the first Brillouin zone of the reciprocal lattice.

When these expansions are substituted into (2) we obtain a system of linear equations for the coefficients $A(\boldsymbol{k}, \boldsymbol{g}_i)$

$$\sum_{\boldsymbol{G}'_i} (\boldsymbol{k} + \boldsymbol{g}_i)(\boldsymbol{k} + \boldsymbol{g}'_i)\tilde{\varepsilon}(\boldsymbol{g}_i - \boldsymbol{g}'_i)A(\boldsymbol{k}, \boldsymbol{g}'_i) = \frac{\omega^2}{c^2} A(\boldsymbol{k}, \boldsymbol{g}_i). \tag{5}$$

Equation (5) has the form of a standard eigenvalue problem with a symmetric matrix, which can be solved numerically to obtain the photonic bandstructure $\omega(\boldsymbol{k})$ and corresponding mode field for any value of $\boldsymbol{k}$. The bandstructure of the E-polarized modes can be obtained in a similar fashion [23]. In other words, the dispersion relations for photonic crystals can be obtained by expressing the spatial distribution of the dielectric constant and the electromagnetic field of the eigenmode in the form of a Fourier series.

We now propose that the spatial variation of the electromagnetic field of the eigenmodes of a quasicrystal should reflect the spatial dependence of the dielectric constant in the structure, and therefore can be represented as a Fourier-like series. Further, it is suggested that we can obtain a good representation of the dispersion relations for the quasicrystal photonic eigenmodes using the Fourier-like series of (1) in place of a true Fourier series as used in the theory of crystals and described by (2)–(5). As the set of RVs for the Fourier representation of the spatial variation of the dielectric constant and eigenmode field, we take the RVs that correspond to the dominant spots in the diffraction pattern.

Such an approach has been applied to the investigation of the bandstructure of photonic Fibonacci lattices. It gives essentially identical bandstructure and transmission spectra to the conventional transfer matrix method if only the branches oriented along the free-photon dispersion line are taken into account. This 'sloped zone' approach can be considered as an analogue of the extended zone scheme analysis for crystals. For crystals there is a periodicity of the dispersion relations in reciprocal space that means that the band structure can be analysed in the first Brillouin zone. In the case of quasicrystals, when such periodicity is absent, the extended zone scheme is more appropriate, since the wavevector of the eigenmode (in first order) is approximately proportional to the wave frequency and average refractive index.

Figure 8 shows dispersion relations calculated using 30 major RVs such as (10000), (10100) and (11000). The branches, oriented along the free-photon lines exhibit two gap-like features. For the E-polarized mode their frequencies are 0.39 and 0.44 for the direction (10010) and 0.375 and 0.47 for the direction (10000). For the H-polarization, the position of the gaps are 0.4 and 0.45 for the direction (10010) and 0.38 and 0.48 for the direction (10000). The relative width of the lower frequency gap is less than 3% for both polarizations and directions while for the upper gap it is about 6% for the direction (10000) and about 3% for the direction (10010). Such behaviour corresponds closely to the transmission spectra. One can see that the dispersion relations, calculated with such a small number of RVs, make the prediction of the position of the gaps with appropriate accuracy possible. Thus the 'free-photon dispersion zone approach' can be used for the prediction of the bandstructure of the quasicrystals. If more RVs are used for the calculation of the dispersion relations, more features appear, reflecting the fractal nature of the band structure of quasicrystalline systems.

Although the width of the gaps for the structure under study are small, they can be increased by increasing the contrast of refractive indices by the use of materials such as silicon nitride, III–V or II–VII semiconductors.

5. Conclusions

The diffraction and transmission of light in Penrose-tiled photonic quasicrystals etched in a silica substrate has been investigated. It was found that for certain frequencies a bandgap

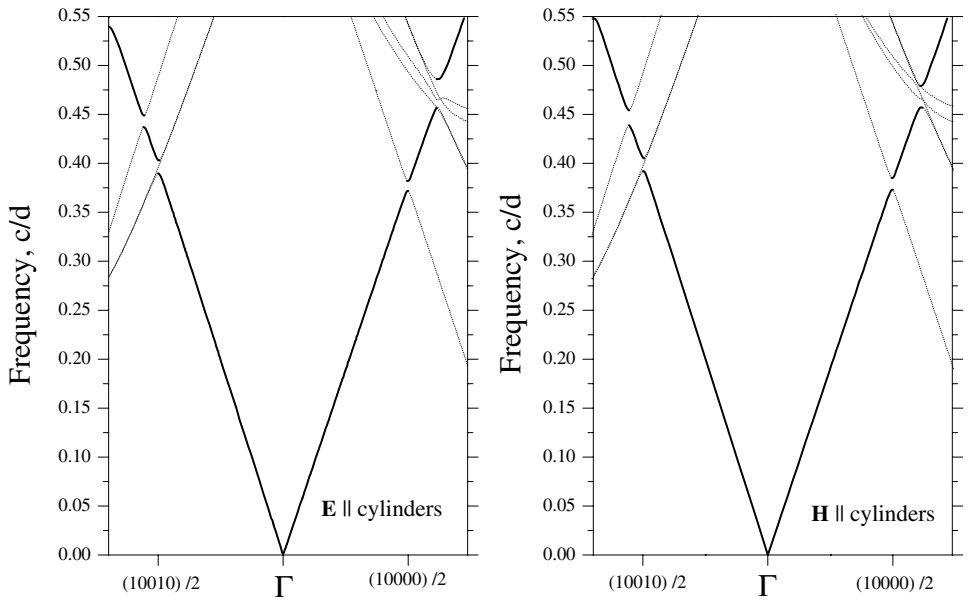

Figure 8. Dispersion relations for photons in the Penrose-tiled photonic quasicrystal, obtained using the major sets of RVs such as (10000), (10100), and (11000). Thick lines highlight the branches, oriented along the free-photon line.

appears for both polarizations and all propagation directions. The 'sloped zone' approach, using a set of RVs taken from the diffraction pattern has been applied for the analysis of the dispersion relation in the two-dimensional Penrose structure, and correspondence between the transmission spectra and dispersion relations has been demonstrated.

Acknowledgments

This work was funded by the EPSRC under grant awards GR/L 73159 and GR/L 73258 and partly by EC, project IST-19996 19009 PHOBOS. The authors thank Professor M G Burt for useful discussions.

References

[1] Joannopoulos J D, Meade R D and Winn J N 1995 *Photonic Crystals: Molding the Flow of Light* (Princeton, NJ: Princeton University Press)
[2] Burstein E and Weisbuch C 1995 *Confined Electron and Photons: New Physics and Devices* (New York: Plenum)
[3] Krauss T F, De La Rue R M and Brand S 1996 *Nature* **383** 699
[4] Yablonovitch E 1987 *Phys. Rev. Lett.* **58** 2059
[5] Janot C 1994 *Quasicrystals: A Primer* (New York: Oxford University Press)
[6] Shechtman D, Blech I, Gratias D and Canh J W 1984 *Phys. Rev. Lett.* **53** 1951
[7] Chan Y S, Chan C T and Liu Z Y 1998 *Phys. Rev. Lett.* **80** 956
[8] Jin C J, Cheng B Y, Man B Y, Li Z L, Zhang D Z, Ban S Z and Sun B 1999 *Appl. Phys. Lett.* **75** 1848–50
[9] Jin C J, Cheng B Y, Man B Y, Li Z L and Zhang D Z 2000 *Phys. Rev.* B **61** 10 762
[10] Kaliteevski M A, Brand S, Abram R A, Krauss T F, De La Rue R M and Millar P 2000 *Nanotechnology* **11** 274–80
[11] Zoorob M E, Charlton M D B, Parker G J, Baumberg J J and Netti M C 2000 *Nature* **404** 740
[12] Zoorob M E, Charlton M D B, Parker G J, Baumberg J J and Netti M C 2000 *Mater. Sci. Eng.* B **74** 168–74

[13] Hattori T, Tsurumachi N, Kawato S and Nakatsuka H 1994 *Phys. Rev.* B **50** 4220–3
[14] Kohmoto M, Sutherland B and Chao Tang 1987 *Phys. Rev.* B **35** 1020–33
[15] Xiujin Fu, Youyan Liu, Peiqin Zhou and Wichit Sritrakool 1997 *Phys. Rev.* B **55** 2882
[16] Kaliteevski M A, Brand S, Abram R A and Nikolaev V V 2001 *Opt. Spectrosc.* **91** 109–18
[17] Carlsson A E 1993 *Phys. Rev.* B **47** 2515
[18] Sabiryanov R F and Bose S K 1994 *J. Phys.: Condens. Matter* **6** 6197
[19] Penrose R 1974 *Bull. Inst. Math. Appl.* **10** 266
[20] Janssen T 1998 *Phys. Rep.* **168** 55
[21] Bell P M, Pendry J B, Martin Moreno L and Ward A J 1995 *Comput. Phys. Commun.* **85** 306–22
[22] Sakoda K 1995 *Phys. Rev.* B **51** 4672
[23] Plihal M and Maradudin A A 1991 *Phys. Rev.* B **44** 8565–71